# Disentangling the viscoelastic properties of bulk polymers from adsorbed polymers using the quartz crystal microbalance

Jurriaan J. J. Gillissen

*Department of Mathematics, University College London, Gower Street, London, WC1E 6BT. E-mail: jurriaangillissen@gmail.com*

Joshua A. Jackman

*School of Chemical Engineering, Sungkyunkwan University, 2066 Seobu-ro, Jangan-gu, Suwon-si, Gyeonggi-do 16419, Republic of Korea.*

Tun Naw Sut, Nam-Joon Cho

*School of Materials Science and Engineering, Nanyang Technological University, 50 Nanyang Avenue 639798, Singapore*

(Dated: August 4, 2019)

# Abstract

At sufficient adhesion energy, polymers may adsorb irreversibly to an interface, with many adhesion sites per polymer and significant changes in their conformation. In addition to irreversibly adsorbing polymers there may be reversibly adsorbing polymers, which are in dynamic equilibrium with bulk polymers, and which have few adhesion sites per polymer and little conformational change. In this work we simultaneously determine the viscoelasticity of irreversibly adsorbed polymers, reversibly adsorbed polymers and bulk polymers. To this end we combine hydrodynamic modelling with quartz crystal microbalance-dissipation (QCM-D) measurements involving an adsorbing target surface and a non-adsorbing i.e. passivated surface. We apply the method to polyethylene glycol adsorption on the water - silica interface. The results demonstrate that the viscoelasticity of the reversibly adsorbing polymers is similar as for the bulk polymers, whereas the irreversibly adsorbed polymers are less elastic. This is the first approach to decouple these viscoelastic contributions, which provides a new analytical tool to quantify the kinetics and conformation of reversibly adsorbing polymers, shedding light on polymer dynamics near interfaces.



Keywords: Polymer adsorption; quartz crystal microbalance; lipid bilayer

## 1. INTRODUCTION

There is broad interest in characterizing the adsorption of biological and synthetic macromolecules towards devising nanoarchitectonic design strategies and achieving functional control over biointerfacial systems [1, 2]. Polymer adsorption at solid-liquid interfaces is governed by the competition between attractive forces, which are small per segment but large per polymer chain, and repulsive, entropic forces, arising from conformational restrictions in the adsorbed state [e.g. 3–6]. Weakly bound, flexible polymers have few conformational restrictions, and consequently their conformation is similar as the random coil in the bulk solution. With an increasing number of bound monomers per polymer, the conformation of the adsorbed polymer chain changes from globular to flattened, and the adsorption becomes irreversible, i.e. dilution of polymers in the bulk solution does not cause polymer desorption from the solid-liquid interface [e.g. 7–9].

In this work, we consider the case, where in addition to strongly bound, irreversibly adsorbed polymers, there are weakly bound, reversibly adsorbing polymers, in dynamic equilibrium with the polymers in the bulk. Since most binding sites are occupied by the irreversibly adsorbed polymers, the reversibly adsorbing polymers bind weakly to the surface with only a few binding sites per polymer, which is referred to as "pinning". Alternatively, reversible adsorption may occur through entanglement with the irreversibly adsorbed polymers [10]. The corresponding configuration is sketched in Fig. 1a, which illustrates irreversibly adsorbed polymers (blue), with trains, tails and loops [4], and reversibly adsorbing polymers (yellow), that are either pinned or entangled, and that are in dynamic equilibrium with the polymers in the bulk (red).

Quantifying reversible adsorption of polymers, that are in dynamic equilibrium with bulk polymers, is challenging, since the measurement is also affected by irreversibly adsorbed polymers and by bulk polymers. Here we combine hydrodynamic modelling with quartz crystal microbalance with dissipation monitoring (QCM-D) measurements, to distinguish between irreversibly and reversibly adsorbed polymers, and bulk polymers. To the best of our knowledge, this de-coupling of effects has not been achieved before, and previous polymer adsorption studies either measured only the irreversible component, or the combined effect of bulk polymers, irreversibly adsorbed polymers and reversibly adsorbed polymers. These previous studies include neutron scattering [11, 12] neutron reflectivity [13], optical

reflectivity [14], infrared spectroscopy [15], nuclear magnetic resonance [16], and QCM-D [9, 17–32].

The QCM-D technique is based on an AT - cut quartz crystal that is piezoelectrically driven to execute oscillations in shear - thickness mode, at its fundamental resonance frequency in the MHz-range and odd overtones thereof [33, 34]. QCM-D measures the change of the resonance frequency $f$ and the damping of the quartz crystal, which occur due to material adsorption, desorption, or phase change [49] at the solid-liquid interface or due to changes of the properties of the bulk solution. The damping of the quartz is usually expressed as the relative energy dissipation per oscillation cycle or in the bandwidth $\Gamma$ of the resonance peak. By measuring the shifts in frequency and bandwidth, QCM-D provides the viscosity and the elasticity, i.e. the viscoelasticity, of the contacting medium. Since the viscoelasticity of a polymer solution is related to the flexibility of the dissolved polymers, QCM-D provides insight into the conformation of the polymer chains.

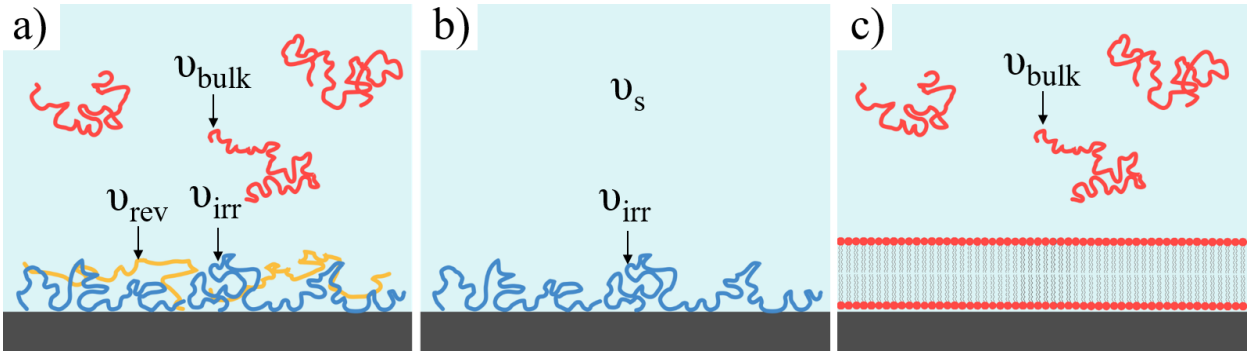


FIG. 1. Irreversibly adsorbed polymers (blue), reversibly adsorbing polymers (yellow), and bulk polymers (red). To measure the viscoelasticity of these three components, we combine three QCM-D experiments. (a) The polymer solution is contacting an uncoated surface, resulting in both irreversibly and reversibly adsorbed polymers. (b) The bulk polymers and the reversible adsorbed polymers are displaced by the pure solvent, and only irreversibly adsorbing polymers remain. (c) The polymer solution is contacting a coated surface, which excludes both irreversibly and reversibly adsorbed polymers.

QCM-D has widely been used to probe the viscoelasticity of polymers, that are either adsorbed on an interface or in the bulk. In this context, we can distinguish between three types of QCM-D experiments, which are illustrated in Fig. 1. In the first type of experiment (Fig. 1a), the polymer solution contacts an adsorbing QCM-D surface, resulting in

irreversibly and reversibly adsorbed polymers, where the latter are in dynamic equilibrium with the bulk polymers. In this case the QCM-D signal is affected by the viscoelasticity of the bulk polymers $\nu_{\mathrm{bulk}}$, but also by that of the irreversible adsorbing polymers $\nu_{\mathrm{irr}}$, and of the reversibly absorbing polymers $\nu_{\mathrm{rev}}$. This type of measurement has been conducted in the literature, where instead of decoupling the different contributions, the corresponding viscoelasticity has been presented as a lumped variable [e.g. 23, 29]. In the second type of experiment (Fig. 1b), the system, that results from the first experiment, is rinsed with pure solvent. The rinsing displaces the bulk polymers as well as the reversibly adsorbing polymers, and the resulting QCM-D signal corresponds only to $\nu_{\mathrm{irr}}$. This type of measurement has been conducted in the literature to study irreversible polymer adsorption [e.g. 9, 21, 22, 25]. In the third type of experiment (Fig. 1c) the polymer solution contacts a surface that is coated with a passivating layer, that excludes both irreversible and reversible polymer adsorption. This type of experiment has been conducted in the literature in order to determine $\nu_{\mathrm{bulk}}$, without the interference of adsorbing polymers [e.g. 30–32, 35].

As mentioned, measuring $\nu_{\mathrm{rev}}$ is challenging, since the QCM-D signal of experiment type one is also affected by $\nu_{\mathrm{irr}}$ and by $\nu_{\mathrm{bulk}}$. Isolating $\nu_{\mathrm{rev}}$, requires subtracting the effects of $\nu_{\mathrm{irr}}$ and $\nu_{\mathrm{bulk}}$, which can be obtained from QCM-D experiments types two and three. This 'subtraction' is non-trivial however and requires hydrodynamic modelling, and has to our knowledge not been achieved so far. In this work we will develop the subtraction rules [Eqs. (11-13) below], and apply these to QCM-D measurements of types one, two and three, in order to, for the first time, simultaneously determine the viscoelasticity of reversibly adsorbing polymers, irreversibly adsorbing polymers, and bulk polymers. Our work thereby extends capabilities of QCM-D to quantify the kinetics and conformation of reversibly adsorbing polymers.

It is noted that previous researchers approximated $\nu_{\mathrm{bulk}}$ in the QCM-D frequency range (10-100 MHz), with viscosity measurements in steady shear flow [9, 17, 18, 26–29]. In this regard, a somewhat better approximation is obtained, by extrapolating dynamic viscosity data, from classical rheometers, which operate at considerably lower frequencies [36]. In comparison to these approximations, we measure $\nu_{\mathrm{bulk}}$ directly in the relevant frequency range (10-100 MHz) using QCM-D.

In this work we apply the above mentioned strategy to QCM-D data for polyethylene glycol (PEG) polymer chains, with a molecular weight of $M_w = 35$ kg/mol, adsorbing onto

a hydrophilic silica surface.

## 2. DATA ANALYSIS

### 2.1. Two Fluid Layer Model

In order to translate the QCM-D measurements into the viscoelasticities of the bulk and the adsorbed polymers, we use known hydrodynamic theory [e.g. 19, 20, 37]. The theoretical setup is sketched in Fig. 2, and consists of two layers, where layer 1 and layer 2 correspond to the adsorption layer and to the bulk, respectively. In the QCM-D experiment, the fluid strain amplitude is less than 1% [34], which implies that the fluid mechanics is in the linear viscoelastic regime. The thickness of the adsorption layer 1 is denoted $\delta$, and the complex kinematic viscosities in layers 1 and 2 are denoted $\nu_1$ and $\nu_2$, and are referred to as viscoelasticities. The viscoelasticity is assumed to follow a box profile, i.e. constant values in the adsorption layer and in the bulk, with a sharp transition at $y = \delta$. This assumption is verified in Fig. 3 below.

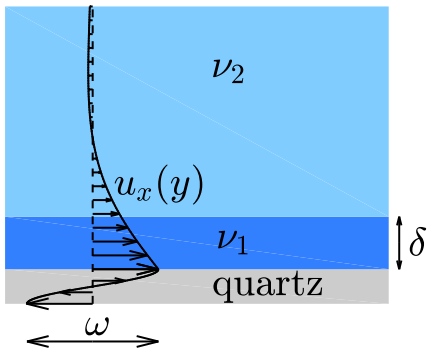


FIG. 2. The hydrodynamic theory assumes two layers of complex fluid, where layer 1 and layer 2 correspond to the adsorption layer and to the bulk, respectively. The thickness of the adsorption layer 1 is denoted $\delta$, and the viscoelasticities in layers 1 and 2 are denoted $\nu_1$ and $\nu_2$. The quartz is oscillating with an angular frequency $\omega$, which results in a dampened viscoelastic wave, with a velocity profile $u_x(y)$.

The theory also assumes, that the fluids are continua, which experience no slip on the wall, and in which the local shear stress is proportional to the local shear rate. This assumption

is reasonable, since the radius of gyration for PEG [38]:

$$R_G/\mathrm{nm} = 0.0215 M_w^{0.583}, \tag{1}$$

which gives $R_G = 10$ nm for a molecular weight of $M_w = 35$ kg/mol, is small compared to the viscous penetration depth $\sqrt{2\nu_s/\omega} = 84$ nm. Here $\nu_s = 10^{-6}$ m$^2$/s is the viscosity of the solvent, $\omega = n2\pi f_0$ is the quartz angular oscillation frequency, $n = 9$ is the overtone, and $f_0 = 5 \times 10^6$ s$^{-1}$ is the base frequency of the quartz. By realising that the thickness of the adsorption layer is bounded by the polymer size $\delta \lesssim R_G$, we see that the system is in the thin-film regime $\delta\sqrt{\omega/(2\nu_s)} \lesssim 1$, which simplifies the modelling [e.g. 34].

Under these assumptions, hydrodynamic theory predicts, that the complex QCM-D frequency shift $\Delta\tilde{f}$ due to an adsorbed layer of viscoelasticity $\nu_1$ and thickness $\delta$ and a bulk fluid of viscoelasticity $\nu_2$ equals [e.g. 19, 20, 37]:

$$\Delta\tilde{f} = \Delta f + \mathbb{i}\Delta\Gamma = \Delta\tilde{f}_{1,\mathrm{box}} + \Delta\tilde{f}_2, \tag{2}$$

where $\mathbb{i} = \sqrt{-1}$. The complex frequency shift is measured relative to the pure solvent, i.e. without polymers, which defines the baseline $\Delta\tilde{f} = 0$. In Eq. (2) $\Delta\tilde{f}_2$ is the (complex) frequency shift due to the bulk alone, i.e. in the absence of the adsorbed layer, which is given by the Kanazawe - Gordon relation [39]:

$$\Delta\tilde{f}_2 = -Q\sqrt{-\mathbb{i}\omega\nu_2^*}, \tag{3}$$

where the asterisk $^*$ denotes complex conjugation. In Eq. (2) $\tilde{f}_{1,\mathrm{box}}$ is the effect of the adsorbed layer, whose viscoelasticity follows a box profile:

$$\Delta\tilde{f}_{1,\mathrm{box}} = -Q\delta\omega\left[1 - \frac{\nu_2^*}{\nu_1^*}\right], \tag{4}$$

which for rigid films $\nu_1 = \infty$ reduces to the well-known Sauerbrey relation $\Delta\tilde{f}_{1,\mathrm{box}} = -Q\delta\omega$ [40]. Here $Q = \rho f_0/(\pi\sqrt{\rho_q\mu_q}) = 125.7$ m$^{-1}$ is a constant related to the quartz crystal and the fluid, $\rho = 10^3$ kg m$^{-3}$ is the fluid mass density, which is assumed constant and equal to that of the solvent, $\rho_q = 2.648 \times 10^3$ kg m$^{-3}$ is the quartz mass density and $\mu_q = 2.947 \times 10^{10}$ kg m$^{-1}$s$^{-2}$ is the quartz shear modulus.

It is noted that, instead of the viscoelasticity $\nu$, the theory [Eqs. (2-4)] can equivalently be formulated using the complex impedance or the complex shear modulus. We use $\nu$ instead, since our focus is on dilute and semi-dilute polymer solutions, where the fundamental material parameter is the solvent viscosity $\nu_s$, i.e. the viscoelasticity of the polymers is of the order of $\nu_s$; see Figs. 7 and 8 below.

## 2.2. Box Profile Assumption

It is emphasised, that Eq. (4) is derived by assuming a box profile for the viscoelasticity, i.e. two flat segments with a sharp transition at $y = \delta$ [e.g. 19, 20, 37]. Here we validate this assumption, by considering the frequency shift due to a smooth viscoelasticity profile $\nu_1(y)$, which is given by the generalisation of Eq. (4) [e.g. 20]:

$$\Delta\tilde{f}_{1,\mathrm{smooth}} = -Q\delta\omega \int_0^\infty \left(1 - \frac{\nu_2^*}{\nu_1^*(y)}\right) dy. \tag{5}$$

To quantify the difference between Eqs. (4) and (5), we assume an exponential profile for $\nu_1(y)$ in Eq. (5), which is consistent with data from neutron experiments [13]:

$$\nu_1(y) = \nu_2 + 2\Delta\nu \exp\left(-2y/\delta\right). \tag{6}$$

Here $\delta$ is the width of the profile:

$$\delta = \frac{\left[\int_0^\infty \left(\nu_1(y) - \nu_2\right) dy\right]^2}{\int_0^\infty \left(\nu_1(y) - \nu_2\right)^2 dy}, \tag{7}$$

and $\Delta\nu$ is the average viscoelasticity excess in the adsorbed layer:

$$\Delta\nu = \frac{\int_0^\infty \left(\nu_1(y) - \nu_2\right)^2 dy}{\int_0^\infty \left(\nu_1(y) - \nu_2\right) dy}. \tag{8}$$

Inserting Eq. (6) into Eq. (5) gives for the smooth profile:

$$\Delta\tilde{f}_{1,\mathrm{smooth}} = -Q\delta\omega\frac{1}{2}\log\left(1 + \frac{2\Delta\nu^*}{\nu_2^*}\right). \tag{9}$$

In order to compare Eq. (9) to Eq. (4), we insert $\Delta\nu = \nu_1 - \nu_2$ into Eq. (4), and find for the box profile:

$$\Delta\tilde{f}_{1,\mathrm{box}} = -Q\delta\omega\left(\frac{1}{1 + \frac{\nu_2^*}{\Delta\nu^*}}\right). \tag{10}$$

In Fig. 3 we plot the relative difference $\left(\Delta\tilde{f}_{1,\mathrm{smooth}} - \Delta\tilde{f}_{1,\mathrm{box}}\right)/\Delta\tilde{f}_{1,\mathrm{box}}$ between the frequency shift due to a smooth viscoelasticity profile $\Delta\tilde{f}_{1,\mathrm{smooth}}$ [Eq. (9)] and due to a box profile $\Delta\tilde{f}_{1,\mathrm{box}}$ [Eq. (10)], as a function of the average, relative, viscoelasticity excess in the adsorbed layer $\Delta\nu/\nu_2$. The present work focusses on $\Delta\nu/\nu_2 \lesssim 1$, and Fig. 3 shows, that under these conditions, the frequency shift, due to a smooth viscoelasticity profile, differs less than 10% from that of a box profile.

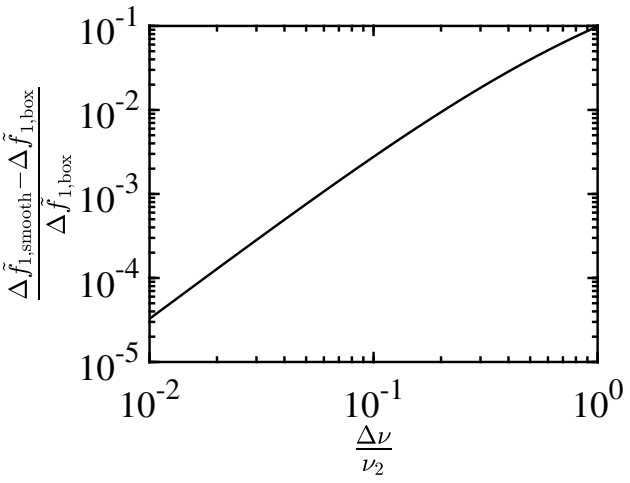


FIG. 3. The relative difference $\left(\Delta\tilde{f}_{1,\mathrm{smooth}} - \Delta\tilde{f}_{1,\mathrm{box}}\right)/\Delta\tilde{f}_{1,\mathrm{box}}$ between the frequency shift due to adsorbed polymers with a smooth viscoelasticity profile $\Delta\tilde{f}_{1,\mathrm{smooth}}$ [Eq. (9)] and with a box profile $\Delta\tilde{f}_{1,\mathrm{box}}$ [Eq. (10)], as a function of the average, relative, viscoelasticity excess in the adsorbed layer $\Delta\nu/\nu_2$.

### 2.3. Working Relations

In this work we determine the viscoelasticity of bulk polymers $\nu_{\mathrm{bulk}}$, and of irreversibly adsorbed polymers $\nu_{\mathrm{irr}}$, and of reversibly adsorbing polymers $\nu_{\mathrm{rev}}$. We extract these three quantities from three (complex) frequency shift measurements, during (i) polymer loading on the uncoated surface $\Delta\tilde{f}_u$, (ii) rinsing, after loading, on the uncoated surface $\Delta\tilde{f}_r$ and (iii) polymer loading on the coated surface $\Delta\tilde{f}_c$. Here the subscripts $u$, $r$ and $c$ refer to "uncoated", "rinsing" and "coated", respectively.

The viscoelasticity of the bulk polymers $\nu_{\mathrm{bulk}}$ is obtained by applying Eq. (3) to the measurement of the (complex) frequency shift during polymer loading on the coated surface $\Delta\tilde{f}_c$. Since $\Delta\tilde{f}_c$ is a measurement w.r.t. the baseline of the pure solvent $\Delta\tilde{f}_s = -Q\sqrt{-\mathbb{i}\omega\nu_s}$, we use that the actual frequency shift (w.r.t. the vacuum baseline) equals $\Delta\tilde{f}_2 = \Delta\tilde{f}_c + \Delta\tilde{f}_s$, where $\nu_s$ is the viscosity of the pure solvent. We furthermore use that the complex viscosity of the bulk $\nu_2 = \nu_s + \nu_{\mathrm{bulk}}$ is due to contributions from the solvent $\nu_s$ and from the bulk polymers $\nu_{\mathrm{bulk}}$. Inserting these expression into Eq. (3) we find for the viscoelasticity of the bulk polymers:

$$\nu_{\mathrm{bulk}} = \frac{\left(\Delta\tilde{f}_c^* + \Delta\tilde{f}_s^*\right)^2}{\mathbb{i}\omega Q^2} - \nu_s. \tag{11}$$

The viscoelasticity of the irreversibly adsorbed polymers $\nu_{\rm irr}$ is obtained by applying Eqs. (2-4) to the measurement of the (complex) frequency shift during rinsing with pure solvent, after polymer loading, on the uncoated surface $\Delta\tilde{f}_r$, which is a measurement w.r.t. the pure solvent baseline, i.e. $\Delta\tilde{f} = \Delta\tilde{f}_r + \Delta\tilde{f}_s$. We furthermore use that the bulk is pure solvent $\nu_2 = \nu_s$ and that the complex viscosity of the adsorption layer $\nu_1 = \nu_{\rm irr} + \nu_s$ is due to contributions from the solvent $\nu_s$ and from the irreversibly adsorbed polymers $\nu_{\rm irr}$. Inserting these expressions into Eqs. (2-4), we find for the viscoelasticity of the irreversibly adsorbed polymers:

$$\nu_{\rm irr} = \nu_s \left[1 + \frac{\Delta\tilde{f}_r^*}{Q\delta\omega}\right]^{-1} - \nu_s. \tag{12}$$

The viscoelasticity of the reversibly adsorbing polymers $\nu_{\rm rev}$ is obtained by applying Eqs. (2-4) to the measurement of the (complex) frequency shift during polymer loading on the uncoated surface $\Delta\tilde{f}_u$, which is a measurement w.r.t. the pure solvent baseline, i.e. $\Delta\tilde{f} = \Delta\tilde{f}_u + \Delta\tilde{f}_s$. We furthermore use that the complex viscosity of the bulk $\nu_2 = \nu_{\rm bulk} + \nu_s$ is due to contributions from the solvent $\nu_s$ and from the bulk polymers $\nu_{\rm bulk}$, and we use that the complex viscosity of the adsorption layer $\nu_1 = \nu_{\rm rev} + \nu_{\rm irr} + \nu_s$ is due to contributions from the solvent $\nu_s$ and from the irreversibly adsorbed polymers $\nu_{\rm irr}$ and from the reversibly adsorbed polymers $\nu_{\rm rev}$. Inserting these expressions into Eqs. (2-4), we find for the viscoelasticity of the reversibly adsorbing polymers:

$$\nu_{\rm rev} = (\nu_{\rm bulk} + \nu_s)\left[1 + \frac{\Delta\tilde{f}_u^* + \Delta\tilde{f}_s^* + Q\sqrt{\mathbb{i}\omega\,(\nu_{\rm bulk} + \nu_s)}}{Q\delta\omega}\right]^{-1} - \nu_{\rm irr} - \nu_s. \tag{13}$$

In Sec. 3 we analyse QCM-D data, by implementing Eqs. (11-13) in the MATLAB software. In the following sub-sections we study the accuracy of this data analysis method, by examining the sensitivity of the outcome of Eqs. (11-13) w.r.t. the assumed film thickness $\delta$ (Sec. 2 2.4) and w.r.t. the QCM-D measurement error (Sec. 2 2.5).

### 2.4. Sensitivity Towards the Film Thickness

Eqs. (12-13) extract the viscoelasticity of the reversibly and irreversibly adsorbed polymers, from QCM-D measurements on adsorbing and non-adsorbing surfaces. Application of these equations requires assuming a value for the adsorption layer thickness $\delta$. This assumption is guided by two physical constraints. First, the size of the adsorbing polymers

can not exceed the size of the bulk polymers, i.e. $\delta \leq 2R_G = 20$ nm for PEG with $M_w = 35$ kg/mol. Second, we use the plausible assumption that the real part $\Re$ of the viscoelasticity of the adsorbing polymers is larger than that of the bulk polymers: $\Re(\nu_{\rm irr} + \nu_{\rm rev}) \geq \Re(\nu_{\rm bulk})$. Inserting this condition in Eq. (13) and using that $Q\sqrt{\mathrm{i}\omega(\nu_{\rm bulk} + \nu_s)} = -\Delta\tilde{f}_c^* - \Delta\tilde{f}_s^*$, gives the following requirement:

$$\delta \geq \frac{-(\Delta f_u - \Delta f_c)}{Q\omega}. \tag{14}$$

Fig. 5 shows that for $M_w = 35$ kg/mol and $n = 9$, $-(\Delta f_u - \Delta f_c)/n \leq 20$ Hz, for all polymer concentrations $c$ considered, which according to Eq. (14) implies, that $\delta \geq 5$ nm $= R_G/2$. When using Eqs. (12, 13) to determine the viscoelasticity of the adsorbed polymers in Sec. 3 3.2, we therefore use an estimated value for $\delta$ in the range $R_G/2 \leq \delta \leq 2R_G$.

It is noted, that in previous work $\delta$ has been obtained by fitting a power-law $\nu_{\rm irr} = an^b$ to the overtone $n$ dependent QCM-D data [41–45]. This approach relies on film resonance effects, which are detectable when the film is sufficiently thick $\delta\sqrt{\omega/[2\Re(\nu_1)]} \geq 0.3$, and requires the full non-linear (in $\delta$) version of Eq. (4). In the present work we are dealing with thin films $\delta\sqrt{\omega/[2\Re(\nu_1)]} \leq 0.2$ which excludes this fitting procedure from being applicable.

Therefore determining $\nu_{\rm irr}$ and $\nu_{\rm rev}$ using Eqs. (11-13) requires estimating $\delta$. We show in Fig. 8 below, that although absolute values of $\nu_{\rm irr}$ and $\nu_{\rm rev}$ depend on the assumed value for $\delta$ within the permissible bounds $R_G/2 \leq \delta \leq 2R_G$, the qualitative trends remain intact. This means that the present approach allows for an accurate determination of the ratio of the viscosity and the elasticity of both $\nu_{\rm irr}$ and $\nu_{\rm rev}$, and of the ratio between $\nu_{\rm irr}$ and $\nu_{\rm rev}$, which are insensitive to the assumed film thickness.

### 2.5. Sensitivity Towards the QCM-D Measurement Error

To study the sensitivity of the method towards the measurement error of the (complex) frequency shift, we apply the method of error propagation [46] to Eq. (12), and relate the error in the viscoelasticity of the irreversibly adsorbed polymers $\nu'_{\rm irr} - \nu_{\rm irr}$ to that of the measured complex frequency shift $\Delta\tilde{f}'_r - \Delta\tilde{f}_r$:

$$\frac{\nu'_{\rm irr} - \nu_{\rm irr}}{\nu_{\rm irr}} \approx \frac{-\left(\Delta\tilde{f}_r^{*\prime} - \Delta\tilde{f}_r^*\right)}{Q\delta\omega}\frac{\nu_s}{\nu_{\rm irr}}\left(\frac{\nu_s + \nu_{\rm irr}}{\nu_s}\right)^2. \tag{15}$$

Using that $\nu_{\rm irr}/\nu_s \sim 10^{-1}$ (Fig. 8) and a QCM-D measurement error of $\Delta\tilde{f}'_r - \Delta\tilde{f}_r \approx 1$ Hz (Fig. 5), we find, that for the $n = 9^{\rm th}$ overtone, the relative error $(\nu'_{\rm irr} - \nu_{\rm irr})/\nu_{\rm irr} \approx 0.02$.

This example illustrates that for relatively soft polymer films $\nu_{\mathrm{irr}}/\nu_s \sim 10^{-1}$, the present method allows for an accurate determination of $\nu_{\mathrm{irr}}$.

In this regard, it is noted that for relatively rigid films $\nu_{\mathrm{irr}}/\nu_s \gg 1$, Eq. (15) predicts much larger relative errors in $\nu_{\mathrm{irr}}$. It has been shown, that accurately measuring the viscoelasticity of such rigid films, requires the use of larger film thicknesses, i.e. $\delta\sqrt{\omega/[2\Re(\nu_{\mathrm{irr}})]} \gtrsim 0.3$, and utilising film resonance effects, i.e. the inclusion of higher order $\delta$-terms into Eq. (4) [41–45].

### 2.6. Sensitivity Towards the Bulk Viscoelasticity

We consider the error, that one would make, when, instead of correctly measuring the viscoelasticity of the bulk polymers $\nu_{\mathrm{bulk}}$, one would assume an erroneous value $\nu'_{\mathrm{bulk}}$. In that case, one would find an erroneous value for the viscoelasticity of the reversibly adsorbing polymers $\nu'_{\mathrm{rev}}$. In order to relate $\nu'_{\mathrm{rev}} - \nu_{\mathrm{rev}}$ to $\nu'_{\mathrm{bulk}} - \nu_{\mathrm{bulk}}$, we apply the methods of error propagation [46] to Eq. (13), where we replace the measured frequency shift on the uncoated surface $-\left(\Delta\tilde{f}_u^* + \Delta\tilde{f}_s^*\right)$ by the theoretical value [Eqs. (2-4)] $Q\sqrt{\mathbb{i}\omega(\nu_{\mathrm{bulk}}+\nu_s)} + Q\sqrt{\omega}\delta[1 - (\nu_{\mathrm{bulk}}+\nu_s)/(\nu_{\mathrm{rev}}+\nu_{\mathrm{irr}}+\nu_s)]$:

$$\frac{\nu'_{\mathrm{rev}} - \nu_{\mathrm{rev}}}{\nu_{\mathrm{rev}}} \approx \left(\frac{\nu'_{\mathrm{bulk}} - \nu_{\mathrm{bulk}}}{\nu_{\mathrm{bulk}}}\right)\frac{\nu_{\mathrm{bulk}}}{\nu_{\mathrm{rev}}}\frac{1}{2\delta}\sqrt{\frac{\nu_s}{\omega}}, \tag{16}$$

and where we have used the thin film approximation $\delta\sqrt{\omega/\nu_s} \lesssim 1$, and that $\nu_{\mathrm{pol}}/\nu_s \lesssim 1$, which is confirmed in Fig. 8. The subscript $_{\mathrm{pol}}$ refers to polymers, that are either in the bulk or irreversibly or reversibly adsorbed on the interface.

If instead of using the correct $\nu_{\mathrm{bulk}}$ obtained from QCM-D [Eq. (11)] we would assume the erroneous value that is measured with a traditional rheometer at zero frequency, we see from Fig. 6 below, that for PEG with $M_w = 35$ kg/mol at $n = 9$ $(\nu'_{\mathrm{bulk}} - \nu_{\mathrm{bulk}})/\nu_{\mathrm{bulk}} \approx 10$. By inserting this value into Eq. (16), we estimate a relative error of $(\nu'_{\mathrm{rev}} - \nu_{\mathrm{rev}})/\nu_{\mathrm{rev}} \approx 30$, where we have furthermore used that for this case $\nu_{\mathrm{bulk}}/\nu_{\mathrm{rev}} \approx 1$ (see Fig. 8 below) and that $\sqrt{2\nu_s/\omega}/(2^{3/2}\delta) \approx 3$, which is based on an adsorption layer thickness of $\delta = R_G = 10$ nm, and a viscous penetration depth of $\sqrt{2\nu_s/\omega} = 84$ nm, which were estimated above. This numerical example illustrates the critical necessity of correctly determining $\nu_{\mathrm{bulk}}$ in order to accurately determine $\nu_{\mathrm{rev}}$.

## 3. EXPERIMENTAL

### 3.1. Frequency and Bandwidth Shifts

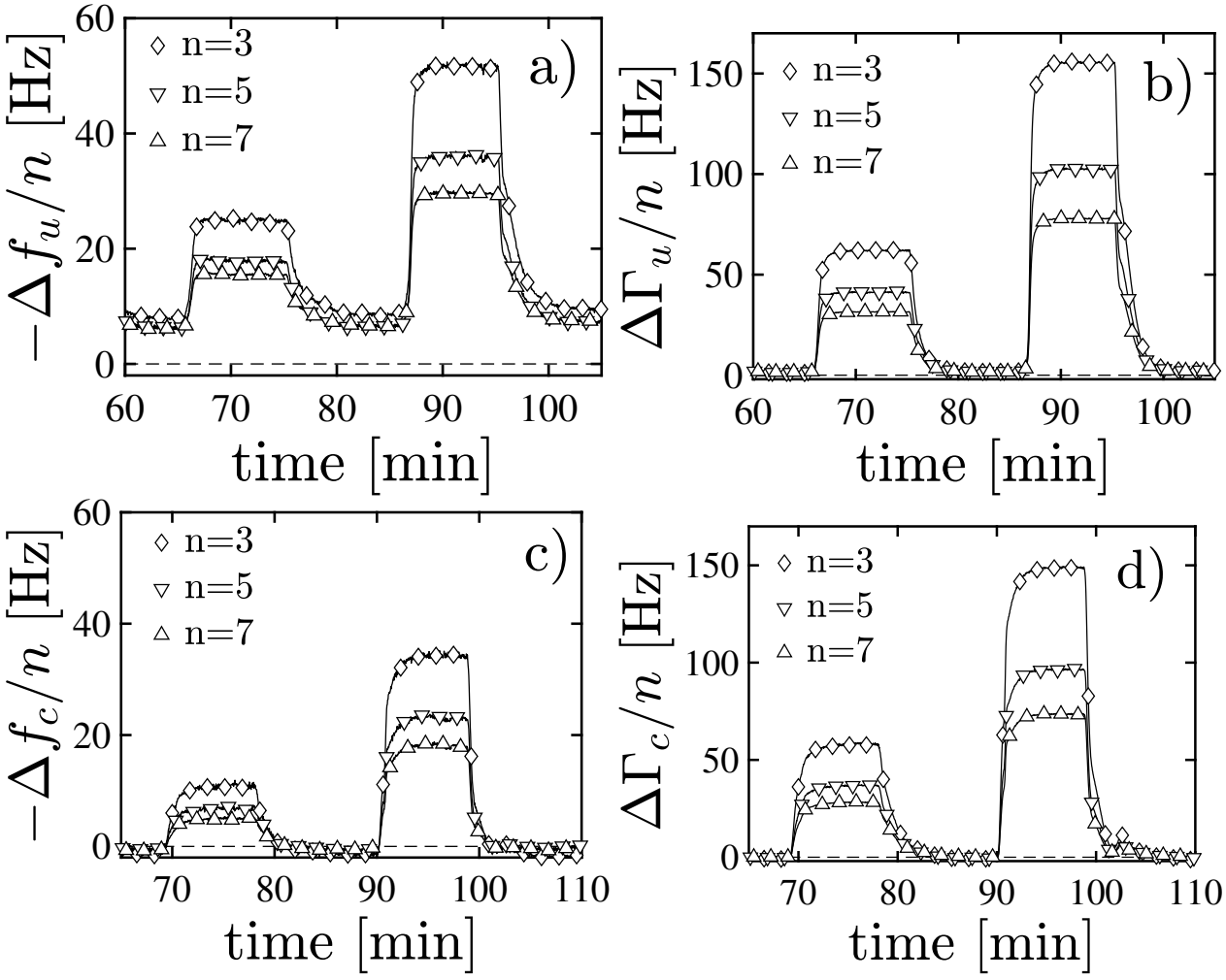


FIG. 4. Time dependent measured frequency shift (a,c) and bandwidth shift (b, d), relative to the baseline of the pure solvent, for solutions of polyethylene glycol (PEG) with a molecular weight of $M_w = 35$ kg/mol contacting a bare silica surface (a, b), and a silica surface that is coated with a supported lipid bilayer (SLB) (c,d), for three selected overtones $n$, during two selected loading steps, corresponding to a polymer bulk concentration of $c = 2\times10^{-2}$ and $c = 5\times10^{-2}$, respectively. The subscripts $u$ and $c$ refer to "uncoated" and "coated" substrates, respectively.

We perform QCM-D experiments using neutral, flexible, and water-soluble polyethylene glycol (PEG) polymer chains with a monomer weight of 44 g/mol and a molecular weight of $M_w = 35$ kg/mol, adsorbing onto a hydrophilic silica surface. The experiments are conducted

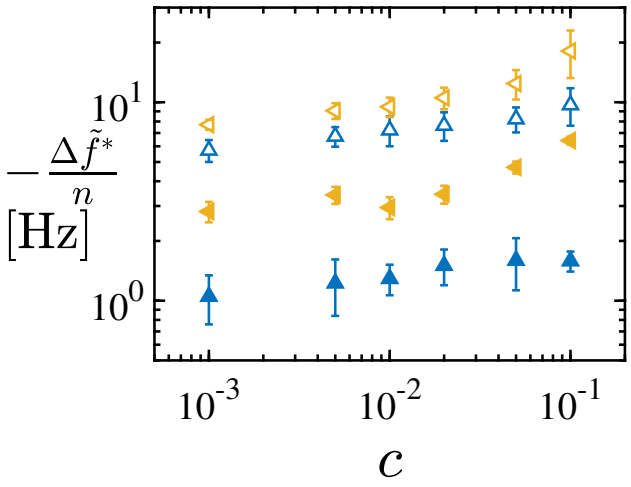


FIG. 5. Negative, real part (open markers) and imaginary part (filled markers) of the complex frequency shift of the irreversibly adsorbed polymers $-\Delta\tilde{f}_r^*$ (blue, upward triangles), and of the reversibly adsorbing polymers $-(\Delta\tilde{f}_u^* - \Delta\tilde{f}_c^*)$ (yellow, leftward triangles), as functions of the bulk polymer concentration $c$, for solutions of polyethylene glycol (PEG) with a molecular weight of $M_w = 35$ kg/mol and for an overtone of $n = 9$.

in deionised water, and the polymer mass fraction in bulk solution is varied between $c = 10^{-3}$ and $10^{-1}$. The volume of the QCM-D measurement chamber equals $V = 58$ mm$^3$, and the volumetric flow rate equals $\dot{V} = 100$ mm$^3$/min, which corresponds to a displacement time of $t = V/\dot{V} = 0.6$ min. The experiment is started with the pure solvent, i.e. without polymer, which defines the baseline. After $t = 10$ min, we switch to $c = 10^{-3}$ polymer solution, which is referred to as "polymer loading", and after another $t = 10$ min, we switch back to pure solvent, which is referred to as "rinsing". Then after another 10 min, we switch to $c = 5 \times 10^{-3}$ polymer solution, and the procedure is continued with increasing polymer concentrations up to $c = 10^{-1}$. All experiments are repeated at least twice.

Figs. 4a, b show the measured QCM-D frequency shift $\Delta f_u$ and bandwidth shift $\Delta\Gamma_u$. Here the subscript $u$ refers to the measurement during polymer loading on the "uncoated", i.e. adsorbing substrate. The results show, that injection of polymer enhances $-\Delta f_u$ and $\Delta\Gamma_u$, which is due to the viscoelasticity of the adsorbed polymers, as well as to that of the bulk polymers. It is further seen that during rinsing, there is a nonzero frequency shift of $-\Delta f_r/n \sim 10$ Hz, where the subscript $r$ refers to "rinsing" after polymer loading. This non-zero signal corresponds to the viscoelasticity of irreversibly adsorbed polymers, that

remain bound during rinsing.

In addition to these irreversibly adsorbed polymers, it is expected, that, during polymer loading, there are also reversibly adsorbing polymers, that are in dynamic equilibrium with the polymers in the bulk. These reversibly adsorbing polymers are either weakly bound to the surface, with just a few binding sites per polymer, referred to as "pinning", or they are unbound to the surface, but entangled with the irreversibly adsorbed polymers [10]. The corresponding configuration is sketched in Fig. 1a, which illustrates irreversibly adsorbed polymers (blue), with trains, tails and loops [4], and reversibly adsorbing polymers (yellow), that are either pinned or entangled, and which are in dynamic equilibrium with bulk polymers (red).

Fig. 5 shows the (complex) frequency shift during rinsing $\Delta\tilde{f}_r$, after loading with increasing polymer concentration $c$ for the $n = 9^{\text{th}}$ overtone. The markers and the error bars in Fig. 5 indicate the average and the difference between two independent measurements. It is observed in Fig. 5, that $\Delta\tilde{f}_r$ increases slightly with $c$, which indicates, that adsorption is nearly, but not entirely, complete during the 10 min polymer adsorption cycles, i.e. after each cycle a few bare spots remain on the substrate, that are progressively being filled in the subsequent cycles. It is important to note, that the main finding of this work does not depend on whether the adsorption is complete or not. The main finding is the decoupling of viscoelasticity of bulk polymers and of irreversibly and reversibly adsorbed polymers.

The (complex) frequency shift during polymer loading on the uncoated surface $\Delta\tilde{f}_u$ is affected by the viscoelasticity of the irreversibly and the reversibly adsorbed polymers and by the bulk polymers, respectively. In order to determine the viscoelasticity of the reversibly adsorbing polymers $\nu_{\text{rev}}$, we need to subtract the viscoelasticity of the irreversibly adsorbed polymers $\nu_{\text{irr}}$, and of the bulk polymers $\nu_{\text{bulk}}$. The $\nu_{\text{irr}}$ is determined from the frequency shift during rinsing $\Delta\tilde{f}_r$, and to determine $\nu_{\text{bulk}}$, we conduct another QCM-D experiment, where, in order to prevent polymer adsorption, the silica surface is coated with a supported bilayer of 1,2-dioleoyl-*sn*-glycero-3-phosphocholine (DOPC) lipids, using the solvent-assisted lipid bilayer formation method [e.g. 47, 48]. Figs. 4c, d show the corresponding (complex) frequency shift $\Delta\tilde{f}_c$ for PEG with $M_w = 35$ kg/mol, where the subscript $c$ refers to polymer loading on the "coated" substrate. In contrast to the frequency shift on the uncoated surface $\Delta\tilde{f}_u$ (Figs. 4a, b), there are no discernible signals during the rinsing steps on the coated surface. This indicates negligible (irreversible and reversible) polymer adsorption on the

303 passivated surface, that is coated with lipid bilayer.

## 304 3.2. Viscoelasticities

### 305 *3.2.1. Bulk Polymers*

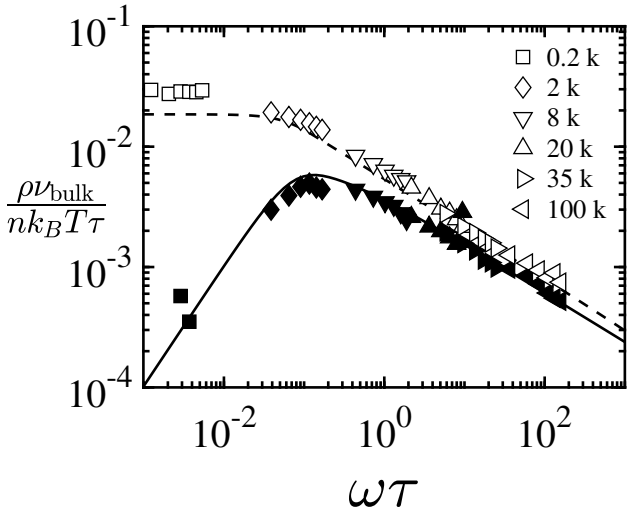


FIG. 6. The real part (open markers) and the imaginary part (filled markers) of the viscoelasticity of polyethylene glycol (PEG) in bulk solution, contacting a silica surface that is coated with a supported lipid bilayer, using various molecular weights $M_w$ (legend), and using a bulk polymer concentration of $c = 10^{-2}$, versus the oscillation frequency $\omega$, which is non-dimensionalised with the bulk polymer relaxation time $\tau$ [Eqs. (1, 17)]. Here $\rho$ is the fluid mass density, $n = cN_A/M_w$ is the polymer number density, $N_A$ is Avogadro's constant and $k_BT$ is the Boltzmann energy. The lines are the predictions of the Zimm model [6].

306 Eq. (11) is used to compute the viscoelasticity of the bulk polymers $\nu_{\rm bulk}$ from the
307 (complex) QCM-D frequency shift during polymer loading on the coated surface $\Delta\tilde{f}_c$ (Fig.
308 4c,d). Fig. 6 shows $\nu_{\rm bulk}$, as a function of the non-dimensional oscillation frequency $\omega\tau$, for
309 PEG molecules with various $M_w$ ranging between 0.2 and 100 kg/mol, and for a fixed bulk
310 polymer concentration of $c = 10^{-2}$. Here $\tau$ is the bulk polymer relaxation time [6]:

$$\tau = 4.78\frac{\rho\nu_s R_G^3}{k_BT}, \tag{17}$$

311 where $\nu_s$ is the viscosity of the pure solvent, and $R_G$ is the radius of gyration, which for PEG
312 is given by Eq. (1). Fig. 6 shows, that for $M_w > 0.2$ kg/mol, the experimental data agree

reasonably well with the Zimm model (lines), which predicts $\nu_{\text{bulk}} \sim \omega^{-1/3}$ at high $\omega$ [6]. For $M_w = 0.2$ kg/mol the discrepancy in the real part of $\nu_{\text{bulk}}$ is probably due to the relatively small polymer size. The corresponding imaginary part has a very small signal to noise ratio, resulting in negative measurement values, which are invisible on the logarithmic scale in Fig. 6. For $M_w > 0.2$ kg/mol the agreement between the measurements and the Zimm model confirms, that there is negligible adsorption of the PEG on the SLB - coated silica surface. The agreement also validates the hydrodynamic assumptions behind Eq. (11), i.e. the polymers are sufficiently small, compared to the viscous penetration depth, such that the polymer solution may be treated as a continuum, and the effect of polymer slip at the quartz surface is negligible.

### *3.2.2. Irreversibly Adsorbed Polymers*

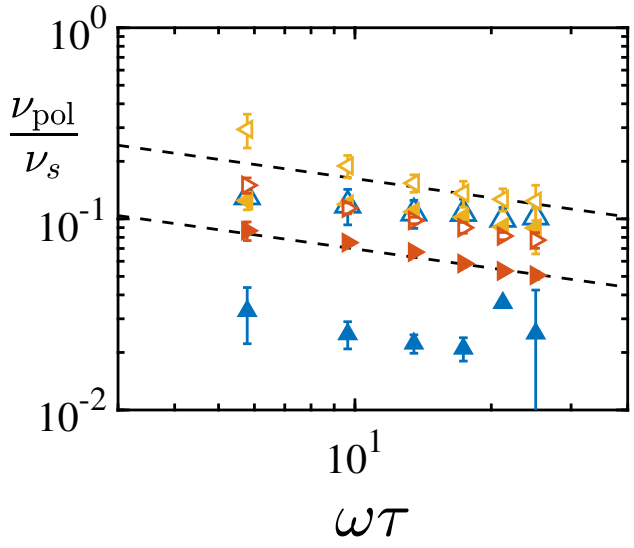


FIG. 7. Real part (open markers) and imaginary part (filled markers) of the viscoelasticity of the bulk polymers $\nu_{\text{bulk}}$ (red, rightward triangles), of the irreversibly adsorbed polymers $\nu_{\text{irr}}$ (blue, upward triangles), and of the reversibly adsorbing polymers $\nu_{\text{rev}}$ (yellow, leftward triangles), scaled with the solvent viscosity $\nu_s$, as functions of the dimensionless frequency $\omega\tau$, for polyethylene glycol (PEG) with a molecular weight of $M_w = 35$ kg/mol and a bulk polymer concentration of $c = 10^{-2}$. The interfacial viscoelasticities $\nu_{\text{irr}}$ and $\nu_{\text{rev}}$ are computed with Eqs. (12) and (13) under the assumption, that $\delta = 2R_G$. The dashed lines have a slope of $-1/3$.

We use Eq. (12) to compute the viscoelasticity of the irreversible adsorbed polymers $\nu_{\mathrm{irr}}$ from the (complex) QCM-D frequency shift during rinsing on the uncoated, bare silica surface $\Delta\tilde{f}_r$ (Fig. 4a, b). To this end, we assume, that the thickness of the adsorption layer $\delta$ equals twice the radius of gyration of the bulk polymers $\delta = 2R_G$.

In Fig. 7 we show the resulting $\nu_{\mathrm{irr}}$, together with the viscoelasticity of the bulk polymers $\nu_{\mathrm{bulk}}$, as functions of the oscillation frequency $\omega$, which is non-dimensionalised with the bulk polymer relaxation time $\tau$ [Eqs. (1, 17)], for a molecular weight of $M_w = 35$ kg/mol and a bulk polymer concentration of $c = 10^{-2}$. The markers and the error bars indicate the average and the difference between two independent measurements. Fig. 7 shows that the ratio $\Re(\nu_{\mathrm{irr}})/\Im(\nu_{\mathrm{irr}})$ of the viscosity (real part $\Re$) and the elasticity (imaginary part $\Im$) is larger than that for $\nu_{\mathrm{bulk}}$. This indicates that the irreversibly adsorbed polymers are less flexible than the bulk polymers, i.e. they have shorter relaxation times, presumably due to the loops of the adsorbed chains, being small compared to the coils in the bulk. This behaviour is consistent with the picture in Fig. 6, showing an increase in $\Re(\nu_{\mathrm{bulk}})/\Im(\nu_{\mathrm{bulk}})$ with decreasing $M_w$. In addition Fig. 7 also shows, that while the viscoelasticity of the bulk polymers follows Zimm scaling $\nu_{\mathrm{bulk}} \sim \omega^{-1/3}$, the viscosity of the irreversibly adsorbed polymers $\Re(\nu_{\mathrm{irr}})$ has a weaker frequency dependence. This behaviour supports the notion of the small loops of the adsorbed chains, which is again consistent with Fig. 6, showing a reduced slope of $\Re[\nu_{\mathrm{bulk}}(\omega)]$ with decreasing $M_w$.

In Fig. 8a we show $\nu_{\mathrm{irr}}$, together with the viscoelasticity of the bulk polymers $\nu_{\mathrm{bulk}}$, as functions of the polymer bulk concentration $c$, for a molecular weight of $M_w = 35$ kg/mol and an overtone of $n = 9$. The markers and the error bars indicate the average and the difference between two independent measurements. It is seen, that $\nu_{\mathrm{irr}}$ is nearly constant, as a function of $c$. As discussed above, the slight increase in $\nu_{\mathrm{irr}}$ with $c$ indicates that adsorption is nearly, but not entirely, complete during the 10 min polymer adsorption cycles.

### *3.2.3. Reversibly Adsorbed Polymers*

We use Eq. (13) to compute the viscoelasticity of the reversibly adsorbing polymers $\nu_{\mathrm{rev}}$ from the (complex) QCM-D frequency shift during polymer loading on the uncoated, bare silica surface $\Delta\tilde{f}_u$ (Fig. 4a, b), where it is still assumed, that $\delta = 2R_G$. The resulting $\nu_{\mathrm{rev}}$ is plotted in Fig. 7, together with the viscoelasticity of the irreversibly adsorbed polymers

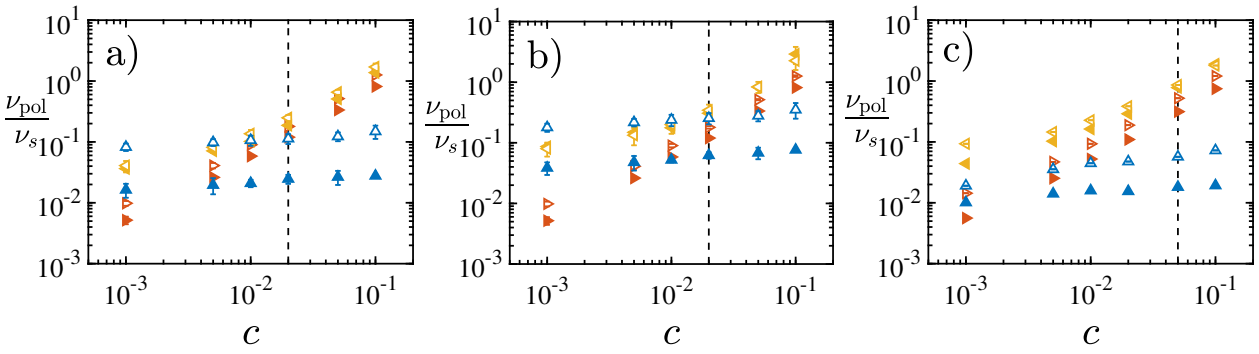


FIG. 8. Real part (open markers) and imaginary part (filled markers) of the viscoelasticity of the bulk polymers $\nu_{\rm bulk}$ (red, rightward triangles), of the irreversibly adsorbed polymers $\nu_{\rm irr}$ (blue, upward triangles), and of the reversibly adsorbing polymers $\nu_{\rm rev}$ (yellow, leftward triangles), scaled with the solvent viscosity $\nu_s$, as functions of the bulk polymer concentration $c$, at an overtone of $n = 9$, for polyethylene glycol (PEG) with a molecular weight of $M_w = 35$ kg/mol (a, b) and $M_w = 8$ kg/mol (c). The interfacial viscoelasticities $\nu_{\rm irr}$ and $\nu_{\rm rev}$ are computed with Eqs. (12) and (13) under the assumption, that $\delta = 2R_G$ (a, c) and $\delta = R_G$ (b). The vertical, dashed lines indicate the polymer overlap concentration $c^*$ [Eq. (18)], which is $c^* \approx 2 \times 10^{-2}$ for $M_w = 35$ kg/mol (a, b) and $c^* \approx 5 \times 10^{-2}$ for $M_w = 8$ kg/mol (c).

$\nu_{\rm irr}$, and of the bulk polymers $\nu_{\rm bulk}$, as functions of the non-dimensional frequency $\omega\tau$ for a molecular weight of $M_w = 35$ kg/mol and a polymer bulk concentration of $c = 10^{-2}$. It is seen, that, similar as for $\nu_{\rm bulk}$ both viscous and elastic components of $\nu_{\rm rev}$ follow Zimm scaling $\nu_{\rm rev} \sim \omega^{-1/3}$. It is furthermore seen, that compared to $\nu_{\rm irr}$, $\nu_{\rm rev}$ has a smaller ratio of the viscosity and the elasticity, and this ratio is close to that of $\nu_{\rm bulk}$. This suggests, that the reversibly adsorbing polymers have a similar viscoelasticity (per polymer) as the bulk polymers. This is consistent with the notion, that reversible adsorption imposes few restrictions on polymer conformation, i.e. their conformation is similar as in the bulk.

In Fig. 8a, $\nu_{\rm rev}$ is plotted as a function of the polymer bulk concentration $c$, for a molecular weight of $M_w = 35$ kg/mol and an overtone of $n = 9$, together with $\nu_{\rm irr}$, and $\nu_{\rm bulk}$. The figure shows that, for small $c$, $\nu_{\rm rev}$ is constant, and when $c$ exceeds a threshold $c^*$, $\nu_{\rm rev}$ increases and approaches $\nu_{\rm bulk}$. The observed $c^*$ is of the order of the polymer overlap concentration:

$$c^* = \frac{M_w}{N_A \rho \frac{4}{3}\pi R_G^3}, \tag{18}$$

which is $c^* = 2 \times 10^{-2}$ for $M_w = 35$ kg/mol. Our data therefore suggest, that for $c \lesssim c^*$, the

reversibly adsorbing polymers form a densely packed layer of non-overlapping coils. This means that the reversible adhesion strength is weaker than the repulsion between overlapping polymer chains. When $c \gtrsim c^*$, the reversible adhesion strength is negligible compared to the pressure between overlapping chains, and the concentration of the reversibly adsorbing chains follows that in the bulk $c$.

Fig. 8b shows the computed interfacial viscosities $\nu_{\rm irr}$ and $\nu_{\rm rev}$ [Eqs. (12) and (13)], by assuming $\delta = R_G$, which is half as large as $\delta = 2R_G$, which was assumed in Fig. 8a. The comparison between Figs. 8a and 8b shows, that the absolute values of $\nu_{\rm irr}$ and $\nu_{\rm rev}$ depend on the assumed $\delta$, but the relative trends remain intact, i.e. the ratio of $\nu_{\rm rev}$ and $\nu_{\rm irr}$ and the ratio of the real and imaginary parts of both $\nu_{\rm rev}$ and $\nu_{\rm irr}$ remain the same, upon changing the assumed $\delta$. This shows that the present method allows for a reliable decomposition of the structure of the adsorbed polymer layer into reversible and irreversible components, and the relative decomposition is insensitive to the assumed value for $\delta$.

We finally show in Fig. 8c the interfacial viscoelasticities $\nu_{\rm irr}$ and $\nu_{\rm rev}$, together with the bulk viscoelasticity $\nu_{\rm bulk}$, computed with Eqs. (11-13) for PEG with a smaller molecular weight of $M_w = 8$ kg/mol. The results are qualitatively the same as for $M_w = 35$ kg/mol (Figs. 8a, b), confirming that the conformation of the reversible adsorbed polymers is similar as that in bulk, while the conformation of the irreversible adsorbed polymers is stiffer. The data also confirm, that the concentration of the irreversibly adsorbed polymers is independent of the bulk concentration $c$, while the concentration of the reversibly adsorbed polymers approaches $c$ for $c \gtrsim c^*$, while it plateaus for $c \lesssim c^*$.

These results therefore consistently demonstrate the ability of the present method to determine the viscoelasticity and thereby the conformation and kinetics of reversibly adsorbing polymers.

## 4. CONCLUSION

We have used the quartz crystal microbalance, to determine the viscoelasticity in the MHz-range of irreversibly and reversibly adsorbing polymers, and of bulk polymers, where the latter two are in dynamic equilibrium with each other. We applied the technique to the adsorption of PEG on the water-silica interface, and thereby find, that the viscoelasticity of the reversibly adsorbing polymers is similar as that for the bulk polymers, whereas the

irreversibly adsorbed polymers have a smaller elasticity relative to their viscosity. The work provides an analytical tool to extract the kinetics and chain conformation of reversibly adsorbed polymers. To our knowledge this is the first approach to decouple the viscoelastic contributions of irreversibly adsorbed, reversibly adsorbed, and bulk polymers in a single system. This capability offers new perspectives on the dynamics of polymers near interfaces.

## COMPETING INTERESTS

The authors declare that they have no competing interests.

## ACKNOWLEDGMENTS

This work was supported by the Engineering and Physical Sciences Research Council of the United Kingdom Grant No. EP/N024915/1, and by a National Research Foundation Proof-of-Concept Grant (NRF2015NRF-POC001-019), and by the Creative Materials Discovery Program through the National Research Foundation of Korea (NRF), that is funded by the Ministry of Science, ICT, and Future Planning (2016M3D1A1024098).

---

[1] M. Komiyama, K. Yoshimoto, M. Sisido, and K. Ariga, B. Chem. Soc. Jpn. **90**, 967 (2017).

[2] J. Guo, J. C. Ho, H. Chin, A. E. Mark, C. Zhou, S. Kjelleberg, B. Liedberg, A. N. Parikh, N.-J. Cho, J. Hinks, *et al.*, Phys.Chem. Chem. Phys. **21**, 11903 (2019).

[3] P.-G. De Gennes, *Scaling concepts in polymer physics* (Cornell University Press, 1979).

[4] J. Scheutjens and G. Fleer, J. Phys. Chem. **83**, 1619 (1979).

[5] P. d. De Gennes, Macromolecules **14**, 1637 (1981).

[6] M. Doi and S. F. Edwards, *The theory of polymer dynamics*, Vol. 73 (Oxford University Press, 1988).

[7] T. Grchev, M. Cvetkovska, T. Stafilov, and J. Schultze, Electrochim. Acta **36**, 1315 (1991).

[8] P. R. Van Tassel, P. Viot, and G. Tarjus, J. Chem. Phys. **106**, 761 (1997).

[9] J. C. Munro and C. W. Frank, Macromolecules **37**, 925 (2004).

[10] J. De Witt and T. Van de Ven, Langmuir **8**, 788 (1992).

[11] A. Karim, S. Satija, J. Douglas, J. Ankner, and L. Fetters, Phys. Rev. Lett. **73**, 3407 (1994).

[12] E. K. Lin, R. Kolb, S. K. Satija, and W.-l. Wu, Macromolecules **32**, 3753 (1999).

[13] T. Cosgrove, T. G. Heath, J. S. Phipps, and R. M. Richardson, Macromolecules **24**, 94 (1991).

[14] R. Longtin, P. Maroni, and M. Borkovec, Langmuir **25**, 2928 (2009).

[15] P. Frantz and S. Granick, Phys. Rev. Lett. **66**, 899 (1991).

[16] T. Cosgrove and J. W. Fergie-Woods, Colloid Surface **25**, 91 (1987).

[17] T. Fu, U. Stimming, and C. Durning, Macromolecules **26**, 3271 (1993).

[18] H. Xu and J. B. Schlenoff, Langmuir **10**, 241 (1994).

[19] M. V. Voinova, M. Rodahl, M. Jonson, and B. Kasemo, Phys. Scripta **59**, 391 (1999).

[20] D. Johannsmann, Macromol. Chem. Phys. **200**, 501 (1999).

[21] A. K. Dutta and G. Belfort, Langmuir **23**, 3088 (2007).

[22] B. Wu, K. Wu, P. Wang, and D.-M. Zhu, J. Phys. Chem. C **111**, 1131 (2007).

[23] P. Wang, J. Fang, Y. Hou, X. Du, and D.-M. Zhu, J. Phys. Chem. C **113**, 729 (2008).

[24] H. Ogi, Y. Fukunishi, H. Nagai, K. Okamoto, M. Hirao, and M. Nishiyama, Biosens. Bioelectron. **24**, 3148 (2009).

[25] A. R. Patel, B. A. Kerwin, and S. R. Kanapuram, J. Pharm. Sci. **98**, 3108 (2009).

[26] M. Yanagioka, M. F. Toney, and C. W. Frank, Macromolecules **42**, 1331 (2009).

[27] S. Qin, X. Tang, L. Zhu, Y. Wei, X. Du, and D.-M. Zhu, J. Colloid Interf. Sci. **383**, 208 (2012).

[28] I. E. Salama, B. P. Binks, P. D. Fletcher, and D. I. Horsup, Colloid Surface A **447**, 155 (2014).

[29] J. Fang, T. Zhu, J. Sheng, Z. Jiang, and Y. Ma, Sci. Rep. **5**, 8491 (2015).

[30] Z. Zhao, X. Ji, R. Dimova, R. Lipowsky, and Y. Liu, Macromolecules **48**, 1824 (2015).

[31] J. Hartl, A. Peschel, D. Johannsmann, and P. Garidel, Phys. Chem. Chem. Phys. **19**, 32698 (2017).

[32] X. Wu, Z. Zhao, Y. Kang, X. Ji, and Y. Liu, Polym. J. **51**, 471 (2019).

[33] I. Reviakine, D. Johannsmann, and R. P. Richter, Anal. Chem. **83**, 8838 (2011).

[34] D. Johannsmann, *The Quartz Crystal Microbalance in Soft Matter Research* (Springer, Basel, 2014).

[35] F. Persson, J. Fritzsche, K. U. Mir, M. Modesti, F. Westerlund, and J. O. Tegenfeldt, Nano Lett. **12**, 2260 (2012).

[36] C. R. Bilchak, Y. Huang, B. C. Benicewicz, C. J. Durning, and S. K. Kumar, ACS Macro Lett. **8**, 294 (2019).

[37] C. C. White and J. L. Schrag, J. Chem. Phys. **111**, 11192 (1999).

[38] K. Devanand and J. Selser, Macromolecules **24**, 5943 (1991).

[39] K. K. Kanazawa and J. G. Gordon II, Anal. Chim. Acta **175**, 99 (1985).

[40] G. Sauerbrey, Z. Phys. **155**, 206 (1959).

[41] G. C. DeNolf, L. Haack, J. Holubka, A. Straccia, K. Blohowiak, C. Broadbent, and K. R. Shull, Langmuir **27**, 9873 (2011).

[42] G. C. DeNolf, L. F. Sturdy, and K. R. Shull, Langmuir **30**, 9731 (2014).

[43] E. J. Martin, M. T. Mathew, and K. R. Shull, Langmuir **31**, 4008 (2015).

[44] E. J. Martin, K. Sadman, and K. R. Shull, Langmuir **32**, 7747 (2016).

[45] K. Sadman, C. G. Wiener, R. Weiss, C. C. White, K. R. Shull, and B. D. Vogt, Anal. Chem. **90**, 4079 (2018).

[46] A. A. Clifford, *Multivariate error analysis: a handbook of error propagation and calculation in many-parameter systems* (Applied Science Publ., London, 1973).

[47] J. J. Gillissen, S. R. Tabaei, and N.-J. Cho, Phys. Chem. Chem. Phys. **18**, 24157 (2016).

[48] A. R. Ferhan, B. K. Yoon, S. H. Park, T. N. Sut, H. Chin, J. H. Park, J. A. Jackman, and N.-J. Cho, Nature Protocols **14**, 2091 (2019).

[49] Y. Okahata, K. Kimura, and K. Ariga, J. Am. Chem. Soc. **111**, 9190 (1989).